Reflectance hyperspectral imaging for colorimetric and spectroscopic studies: the analysis of an impressionist painting.

Alice Pertica[1], Andrea Casini[1], Costanza Cucci[1], Marcello Picollo[1], Lorenzo Stefani[1], Muriel Vervat[2]

[1] IFAC-CNR, Via Madonna del Piano 10, 50019 Sesto Fiorentino (FI), Italy

[2] Studio Muriel Vervat, Via dei Velluti 29r, 50125 Firenze, Italy

Corresponding author: Alice Pertica (alicepertica@gmail.com)

ABSTRACT

In the last few years reflectance hyperspectral imaging (HSI) has been increasingly employed in the study of cultural heritage and its conservation. HSI systems acquire hundreds of images in narrow contiguous spectral bands in the visible (400-750 nm) and near infrared (750-2500 nm) spectral regions. These form a tridimensional data set called “cube-file”: the two coordinates x and y are associated to the spatial information, while the third one to the spectral information. By manipulating this cube-file it is possible to obtain different kind of information: reflectance spectra, colorimetric data, and images at different spectral bands (or range).
In particular, this article will focus on the combination of colorimetric and spectroscopic analyses for the study of artworks, with the final aim of highlighting the colorimetric differences between different pigments. To reach this goal, a 19th century easel painting was analyzed with a HSI system developed at the “Nello Carrara” Institute of Applied Physics. Starting from the cube-file, it was possible to extract the reflectance spectra for different areas of color and to calculate the colorimetric values for these pixels. Therefore, the materials were identified, and this allowed to compare the different shades of hues – obtained with different pigments – with their colorimetric values.

KEYWORDS reflectance hyperspectral imaging, spectroscopy, colorimetry, conservation science, easel painting.

RECEIVED 31/03/2023; **REVISED** 30/07/2023; **ACCEPTED** 09/08/2023

1. Introduction

Reflectance hyperspectral imaging (HSI) is a relatively new technique, originally developed for remote sensing and astrophysics (Ming *et al.*, 1993; Nieke *et al*., 1997; Mouroulis *et al*., 1998). Nowadays it is increasingly employed in the field of art conservation science, for the analysis and the documentation of artworks. HSI is a non-invasive technique, which consists in the acquisition of hundreds of images in spectral bands that are narrow and contiguous, usually with a bandwidth less than 10 nm. These bands can belong to the visible (Vis 400-750 nm) and/or near infrared (NIR 750-2500 nm) spectral regions [1] (Verhoeven, 2018). These images together form a tridimensional data set known as "cube-file", in which the two coordinates x and y represent the spatial information, while the third dimension contains the spectral information (λ, wavelength). By manipulating these cube-files it is possible to obtain several different kinds of information. Firstly, it is possible to extract images at different wavelengths for every spectral band (or range): it permits to detect potential underdrawings, restorations, *pentimenti*, damages and other hidden details. Secondly, the extraction of a reflectance spectrum for each pixel of the image allows – potentially – identifying the pigments and other materials employed by the artists (Cucci, *et al.*, 2016; Picollo, *et al*., 2020; Striova, *et al*., 2020). Moreover, it is possible to calculate the colorimetric values for each pixel, but only if the measurement geometry follows the recommendations given by the International Commission on Illumination (CIE) (CIE, 2004; Picollo *et al.*, 2023). These values are obtained following the calculation procedures that are provided by the CIE (Marcus, 1998; Berns, 2001; Burger & Burge, 2009). Lastly, it is very important to remember that also the application of algorithms could help to find other details or information about the artistic technique (Cucci, *et al.*, 2016; Picollo, *et al*., 2020; Striova, *et al*., 2020).

In addition, the HSI systems have been employed in the analysis of different works of art, from easel and mural paintings to paper artefacts (Cucci, *et al.*, 2015; Cucci, *et al*., 2016; Delaney *et al.* 2016; Mounier & Daniel, 2017), artistic glass (Perri, *et al.*, 2019; Palomar, *et al.*, 2019) and photographic films (Picollo, *et al.*, 2020; Cucci, *et al.*, 2023).

Everything considered, it is now evident how hyperspectral imaging is a very versatile instrument for the non-invasive investigation and documentation of different kinds, mainly 2D, of cultural heritage objects.

In this paper, the focus will be the combination of reflectance spectroscopy and colorimetry. They are two non-invasive techniques that are often employed in the analysis of artworks (Bacci, 2000; De la Roja, *et al*., 2007; Lorusso, *et al*., 2007; Gil, *et al*., 2014). With hyperspectral imaging these methodologies can be carried out by using just one instrument. Therefore, one of the aims of this work is to demonstrate the versatility and the usefulness of this instrument to study the hues of color and the used materials. The hyperspectral system employed to reach this goal is the one designed and developed at the "Nello Carrara" Institute of Applied Physics (Florence, Italy). Specifically, it was used to analyze a 19th century painting: the final aim is in fact to highlight the colorimetric difference between different pigments of the same color, by comparing and connecting the materials to the shades of hue.

2. Method

2.1. *Case study*

The 19th century easel painting (24.5×32.6 cm, private collection) represents a floral composition, with roses, probably peonies and a wood log (Fig. 1). It dates back to the impressionist period and it has the signature – on the bottom left corner – of the famous painter Édouard Manet (Paris, 1832-1883).

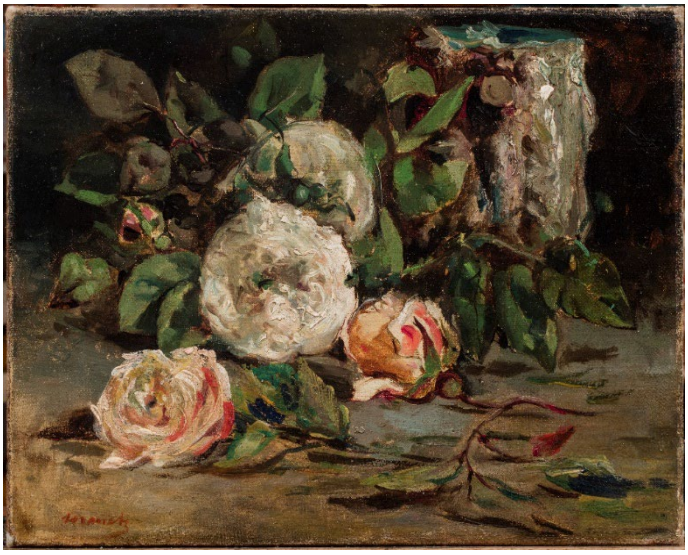

Fig. 1. The analyzed painting

Starting from the acquired cube-files, it was possible to obtain the reflectance spectra for selected pixels of the image – chosen among the different areas of color – to tentatively identify the pigments that composed the artist's color palette. Instead, the values of the colorimetric coordinates for the same pixels were calculated in the CIE L*a*b* 1976 color space (Burger & Burge, 2009). Subsequently, these data were compared among them to find the colorimetric difference between different pigments.

2.2. *Experimental*

The hyperspectral system employed in this study was designed and developed at IFAC-CNR. It is composed of two hyperspectral heads that are alternatively mounted on

a moving mechanical structure (for pushbroom scanning). One head works between 400 and 900 nm (visible and near-infrared, VNIR), with a telecentric objective (Opto-Engineering Srl) and a prism-grating-prism (PGP) line-spectrograph (Specim ImSpector™ mod. V10E) connected with a digital CCD camera (Hamamatsu CCD ORCA-ERG) (Cucci, *et al.*, 2011). The other head operates between 950 and 1650 nm (short-wave infrared, SWIR), with a telecentric objective, a PGP line spectrograph (Specim ImSpector™ mod. N17E) and a digital camera with an InGaAs array (Xenics® mod. Xeva 1.7-640) (Cucci, *et al.*, 2013).

The illumination module consists in two fiber optics illuminators which are fixed to the scan-head so as they light the artwork with an angle of 45°. This is essential to obtain a 45°/0° illumination/observation geometry, suitable for colorimetric analyses. The radiation comes from a Quartz Tungsten Halogen lamp (QTH, 150 W, 3200 K) equipped with a thermal filter during visible measurements, replaced with a filter which blocks visible radiation for SWIR measurements.

This instrument has high spatial and spectral resolutions. The spatial sampling is 11.4 points/mm in the VNIR region and 9.2 points/mm in the SWIR setup. The spectral sampling of the VNIR cube is 1.25 nm, with 400 bands and a spectral resolution of 2.5 nm. The second cube, the SWIR one, has a spectral sampling of 2.1 nm, with 332 bands and a spectral resolution of 6 nm. At the end, two cube-files are obtained, with a total of 732 spectral bands from 400 to 1650 nm.

The obtained cube-files were manipulated using ENVI®, a software designed for hyperspectral images processing and analysis. The reflectance spectra were firstly visualized with ENVI®, saved as .txt files in order to process them with Origin 6.0, a graphing and data analysis software.

The colorimetric values were calculated from the reflectance spectra with programs developed specifically for this aim at IFAC (Picollo, *et al.*, 2020; Cherubini, *et al.*, 2023). The colorimetric images – extracted from the hyperspectral ones – contain the L*, a*, b* values for the CIE 1931 2° Standard Observer with illuminant D65, reported as separated floating point TIFF images, which can be displayed and analyzed with image processing programs, in this case they were obtained using Fiji – ImageJ.

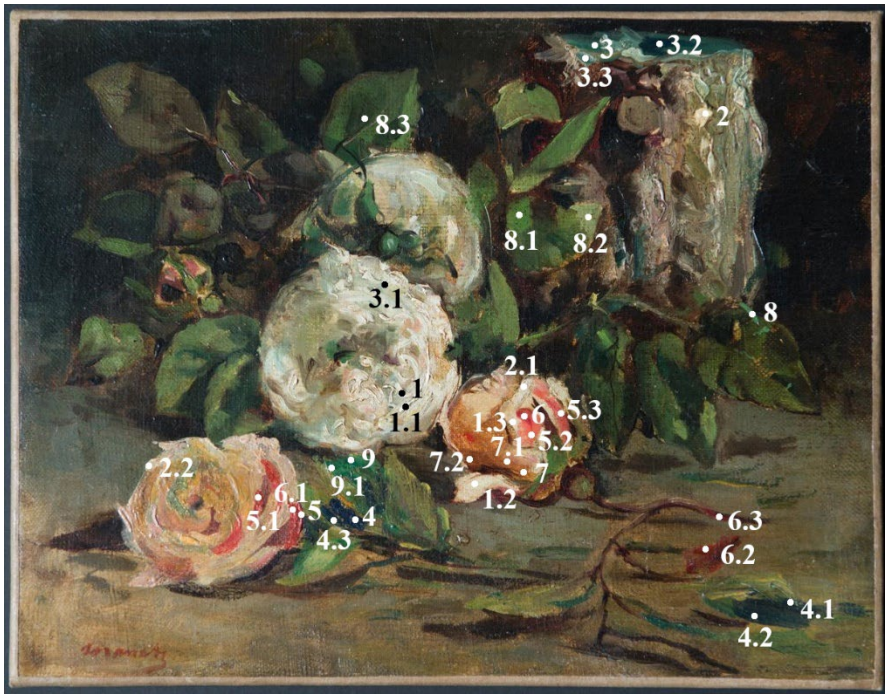

Fig. 2. The points from which the reflectance spectra were extracted.

3. Results

The selected points from which the reflectance spectra were extracted and the colorimetric coordinates calculated are displayed in Fig. 2. The first ones were obtained from the cubes (from an area of 5×5 pixels [2], 0.44×0.44 mm for the VNIR cube) and analyzed to identify the materials by using the SABeC IFAC-CNR Spectral Database (https://spectradb.ifac.cnr.it) and references from the literature. Instead, the colorimetric values were reported in the L*a*b* 1976 color space.

In the following paragraphs the results will be presented divided according to the areas of color.

POINT	PIGMENT	L*	a*	b*
1	Lead white	80.82	0.18	21.64
1.1	"	85.44	2.09	18.53
1.2	"	76.61	-1.21	30.17
1.3	"	69.64	5.06	23.66
2	Lithopone	74.23	2.79	27.05
2.1	"	73.83	3.58	27.30
2.2	"	74.05	-0.31	19.23

*Table 1. CIE L*a*b* 1976 values for each point of the white areas and their pigment attribution.*

3.1. *White areas*

The white pigment mostly employed by the artist is lead white (basic lead carbonate ($PbCO_3)_2 \cdot Pb(OH)_2$), but there are some areas – some brushstrokes and the flower in the left corner – that are made with lithopone (mixture of barium sulfate, $BaSO_4$, and zinc sulfide, ZnS).
The first one was identified thanks to the absorption band at 1445 nm (first OH stretching overtone) visible in the SWIR spectrum. Instead, lithopone shows absorption bands at 650 nm and 730 nm, due to the presence of cobalt ions as substituents of the sulfur ion in the zinc sulfide (Fig. 3). This type of lithopone belongs to the improved version of pigment developed in the 1920s (Bacci, et al., 2007): this and the fact that this pigment is used only in restricted areas might be attributable to following retouching.

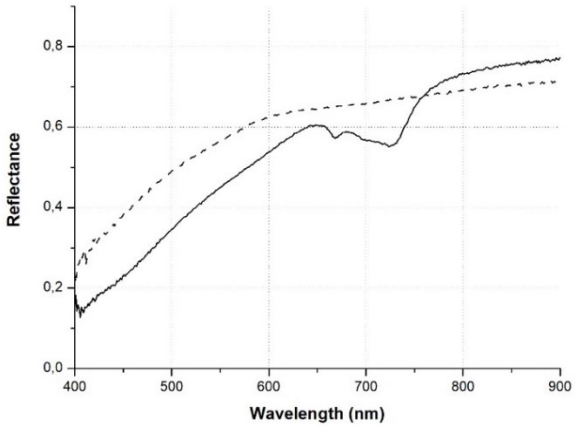

Fig. 3. Reflectance spectra of lithopone (solid line, point 2) and lead white (dash line, point 1) (AVG 5×5).

From a colorimetric point of view (Table 1), both pigments have a high value of L*, since they are white pigments with a high brightness. However, lithopone has higher a* and b* values (more red and yellow components) than lead white, resulting in a warmer hue. This yellowing effect is evident even to the naked eye and might be due to a differentiated aging than other white zones.

3.2. *Blue areas*

The blue areas are made with two different pigments: in the upper part of the painting the artist employed Prussian blue (ferric ferrocyanide, $Fe_4[Fe(CN)_6]_3$), while in the lower part some zones are obtained with the ultramarine blue (lapis lazuli, $Na_{8-10}Al_6Si_6O_{24}S_{2-4}$).
The reflectance spectrum of Prussian blue shows an absorption band at 730 nm, whereas ultramarine has an absorption band at 600 nm and both transitions are due to charge-transfer processes (Fig. 4) (Bacci, 2000; Aceto, *et al.*, 2014).

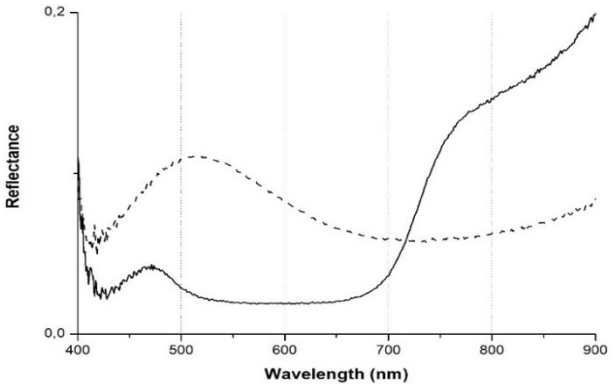

Fig. 4. Reflectance spectra of ultramarine blue (solid line, point 4) and Prussian blue (dash line, point 3) (AVG 5×5).

Since the artist used ultramarine blue to depict some shadows, the resulting color is quite dark, with low values of L*. On the contrary, Prussian blue was employed to obtain different shades of blue, from the brightest in the central flower to the darkest in the wooden log. For example, point 3.1 is a very light blue, while point 3.2 is darker, with L* values similar to ultramarine. In general, this pigment has more green and yellow components than ultramarine blue, in fact every point has a positive value of b*, that is far from the usual values of a blue pigment. For instance, point 3 shows a more greenish hue, also evident from the value of a* (Table 2).

POINT	PIGMENT	L*	a*	b*
3	Prussian blue	32.51	-17.07	7.97
3.1	"	57.63	-5.94	9.82
3.2	"	18.21	-7.61	1.32
3.3	"	35.95	-9.90	4.29
4	Ultramarine blue	10.28	-2.31	-9.20
4.1	"	24.22	-3.54	-1.86
4.2	"	18.44	-3.60	2.72
4.3	"	15.15	-3.78	-0.31

*Table 2. CIE L*a*b* 1976 values for each point of the blue areas and their pigment attribution.*

3.3. *Red areas*

To obtain shades of red the artist used vermilion (mercury sulfide, HgS) and a red lake. The first one shows a typical sigmoid-shaped spectrum with an inflection point at around 600 nm due to band-to-band transition. The red lake shows a similar sigmoidal trend, although with a less steep rise after the inflection point (Fig. 5). It was not possible to define its origin (vegetal or animal) because the typical absorption bands in the 500-580 nm range are not visible (Aceto, *et al*., 2014; Vitorino, *et al*., 2015).

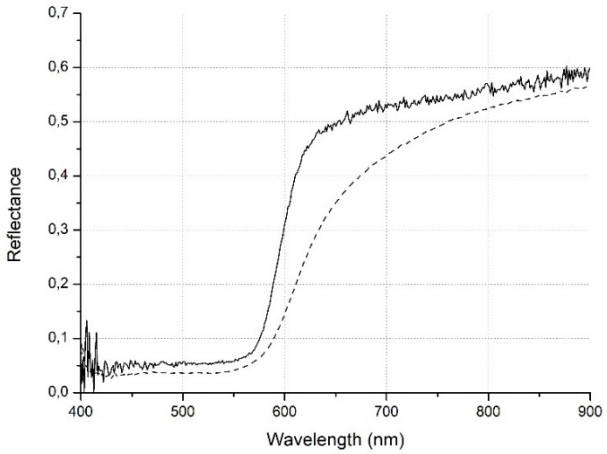

Fig. 5. Reflectance spectra of vermilion (solid line, point 5) and red lake (dash line, point 6) (AVG 5×5).

Colorimetric data (Table 3) show that the areas painted with vermilion seem to be more vivid than the one with the red lake (higher L* values). In general, it has a colder hue, because of the lower b* values. Nevertheless, there are still some areas that show different shades, such as point 5.2 (vermilion) that has a higher component of yellow compared to the other points. For what concerns the red lake, instead, point 6.2 has a higher value of b* than the other points, while 6.3 has a very low value of this coordinate, which means a less yellow component. This can be due to the influence of a darker pigment below the lake in this area.

POINT	PIGMENT	L*	a*	b*
5	Vermilion	41.90	39.25	19.52
5.1	"	36.10	33.63	19.59
5.2	"	48.31	36.57	31.00
5.3	"	44.39	35.64	23.17
6	Red lake	29.77	38.50	26.43
6.1	"	31.89	38.77	28.09
6.2	"	28.98	40.55	40.72
6.3	"	24.23	29.68	14.80

*Table 3. CIE L*a*b* 1976 values for each point of the red areas and their pigment attribution.*

3.4. *Brown areas*

An iron oxide pigment (Fe_2O_3) was used to create brownish areas and shadows. This pigment is identifiable from the absorption band in the reflectance spectra at 550 nm caused by charge-transfer transitions, the shoulder at 680 nm and the band at 850 nm, both due to ligand field transitions (Fig. 6) (Aceto, et al., 2014).
Since it is a brown pigment, it shows high values of red and yellow components (respectively a* and b*) (Table 4).

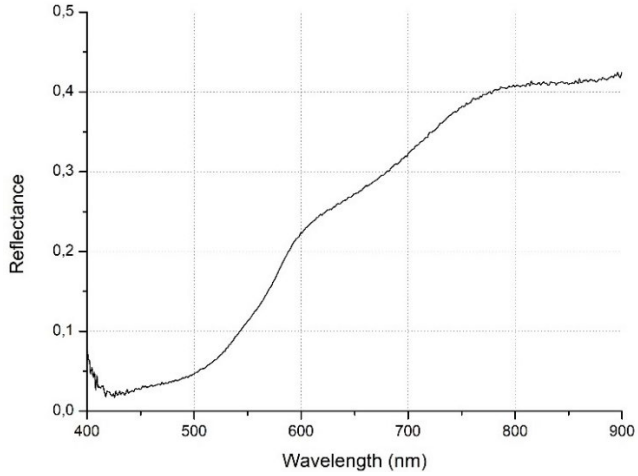

Fig. 6. Reflectance spectra of iron oxide pigment (point 7) (AVG 5×5).

POINT	PIGMENT	L*	a*	b*
7	Iron oxide pigment	39.18	21.67	37.65
7.1	"	41.54	24.75	38.22
7.2	"	27.93	19.33	26.06

*Table 4. CIE L*a*b* 1976 values for each point of the brown areas and their pigment attribution.*

3.5. *Green areas*

The green pigment that is employed in almost the entire painting is a mixture of Prussian blue and a yellow pigment (that could be chrome yellow – lead chromate – $PbCrO_4$). Nevertheless, there are some leaves in the bottom left part of the painting that are obtained with another green pigment. In fact, this one shows a different reflectance spectrum (Fig. 7), but it was not possible to identify it, even though it may be a chromium-based pigment, according to the shape of the spectrum between 450 and 800 nm. The mixture has higher values of L* than the other green pigment, except for point 8.3 that refers to a darker area, with lower values of a* and b*, which translates to a minor presence of green and yellow in the color. Moreover, the unidentified green shows lower b* values which means that this pigment results colder than the mixture of Prussian blue and yellow.

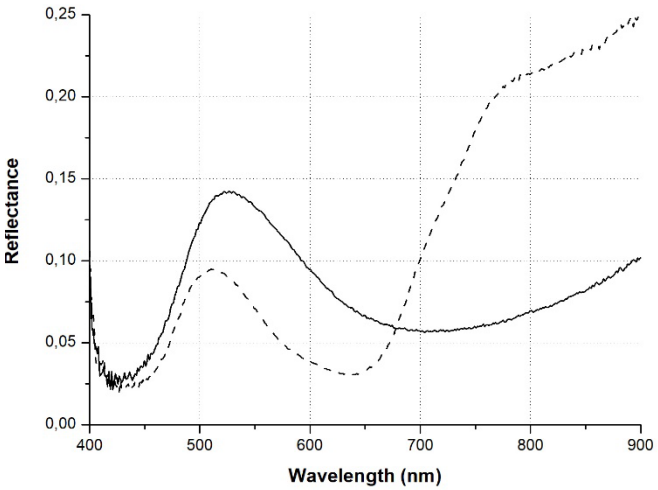

Fig. 7. Reflectance spectra of mixture of Prussian blue and yellow (solid line, point 8) and unidentified green pigment (dash line, point 9) (AVG 5×5).

POINT	PIGMENT	L*	a*	b*
8	Prussian blue + yellow	40.65	-20.83	24.12
8.1	"	37.25	-18.14	26.86
8.2	"	49.31	-6.33	21.77
8.3	"	27.67	-6.46	10.78
9	Unidentified green	32.83	-24.43	15.84
9.1	"	32.51	-29.61	16.16

*Table 5. CIE L*a*b* 1976 values for each point of the green areas and their pigment attribution*

4. Conclusion

This study – among the others – shows how HSI is a very useful tool in the study of artworks and their materials. In this case, it was possible to obtain the colorimetric data and the reflectance information by manipulating the hyperspectral cube-files (Picollo, *et al.*, 2020; Cherubini, *et al.*, 2023). The combination between them allowed to highlight and understand the differences in the tones between different pigments used to create the same color. To summarize, in the whites the presence of lithopone is evident – apart from their reflectance spectra – from the more yellow hue than the lead white that can be imputed to following retouching. In blue areas, ultramarine blue is used almost pure to realize very dark shadows, while Prussian blue is employed with different shades, but in general with a greener hue. The red details are created with vermilion and the glazes with a red lake; the first one it is more vivid and cold than the second one. On the other hand, brown shadows and areas are obtained with an iron oxide pigment which shows higher values of red and yellow in its colorimetric coordinates. The green hues are depicted by using a mixture of Prussian blue and yellow and probably a chromium-based pigment: the first one is used with different shades, while the second is used only in a restricted area of the painting and appears colder than the mixture.
In conclusion, HSI is very powerful non-invasive technique that can potentially provide various information about the works of art, the materials of which they are made of and their artistic production technique.

5. Conflict of interest declaration

The authors state that no actual or potential conflict of interest exist with other people or organizations.

6. Funding source declaration

The authors state that no external funding has been involved in this study.

7. Short biography of the authors

Alice Pertica - graduated in Science and materials for conservation and restoration of cultural heritage at the University of Florence. Her interests include non-invasive investigation of cultural heritage.

Andrea Casini - MSc in Physics in 1968, has been a researcher at IFAC-CNR from 1972 to 2010. Expert in signal and image processing, for many years he has been developing imaging spectroscopic methodologies for the study of works of art in the "Integrated spectroscopic methods for the diagnostics and monitoring of cultural and environmental heritage" project, with which he continues to collaborate as associate researcher.

Costanza Cucci - got her Physics "Laurea" and Ph.D. in Conservation Science at the Florence University. Currently she is a researcher at IFAC-CNR. Her research focus is on spectroscopic techniques and data-processing algorithms applied to the fields of cultural heritage, environmental monitoring, and safety food controls.

Marcello Picollo - Ph.D., is a researcher at IFAC-CNR. His interests include color measurement, Vis-NIR Hyperspectral Imaging, and spot size UV-Vis-IR spectroscopic investigations of 2D polychrome objects.

Lorenzo Stefani - is a technician in telecommunications at IFAC-CNR. He is in charge of the development of hardware and software for computer-controlled instrumentation for the non-invasive and in situ study of artworks.

Muriel Vervat - Graduated from the Higher Education School of the Opificio delle Pietre Dure in 1983, she carried out a professional activity in the sector of the restoration of paintings on wood and canvas. She is included in the list of restorers of cultural heritage of the MiBACT.

Notes

[1] This division into spectral ranges is the one used in the spectroscopy field. Instead, in the field of detectors it is slightly different (see section 2.2.).

[2] The resulting spectra are the average of every spectrum of each pixel in this area of 5×5 pixels. In the following paragraphs the term “AVG 5×5” will refer to this average.

Licensing terms

References

Aceto, M. *et al*. (2014). ‘Characterisation of colourants on illuminated manuscripts by portable fibre optic UV-visible-NIR reflectance spectrophotometry’, *Analytical Methods*, 6, pp. 1488-1500. doi: 10.1039/c3ay41904e.

Bacci, M. (2000). ‘UV-VIS-NIR, FT-IR, and FORS spectroscopies’. In: E. Ciliberto & G. Spoto, eds. *Modern Analytical Methods in Art and Archaeology*. John Wiley and Sons, Inc., pp. 321-361.

Bacci, M. *et al*. (2007). ‘Non-invasive identification of white pigments on 20th-century oil paintings by using fiber optic reflectance spectroscopy’, *Journal of the American Institute for Conservation*, 46(1), pp. 27-37. doi: 10.1179/019713607806112413.

Berns, R. S. (2001). ‘The Science of Digitizing Paintings for Color-Accurate Image Archives: A Review’, *Journal of Imaging Science and Technology*, 45(4), pp. 305−325.

Burger, W. & Burge, M. J. (2009). ‘Colorimetric Color Spaces’. In: Mackie, I., Ed., ‘Principles of Digital Image Processing’, *Undergraduate Topics in Computer Science*, chapter 6, pp. 97-124. doi: 10.1007/978-1-84800-195-4_6.

Cherubini, F. *et al.* (2023). ‘Application of a hyperspectral camera for colorimetric measurements on polychrome surfaces in a controlled environment and evaluation of three image processing software for displaying colorimetric data: Pros and cons of the methodology presented’, *Color Res Appl.*, 48, pp. 210–221. doi: 10.1002/col.22835

CIE (2004). ‘Technical Report. Colorimetry’, 3rd Edition, Vienna: Commission International de l’Eclairage (CIE).

Cucci, C. *et al*. (2011). ‘Open issues in hyperspectral imaging for diagnostics on paintings: when high spectral and spatial resolution turns into data redundancy’, *Optics for Arts, Architecture and Archaeology, SPIE*, 8084(III), pp. 1-10. doi: 10.1117/12.889460.

Cucci, C. *et al*. (2013). ‘Extending Hyper-Spectral Imaging from Vis to NIR spectral regions: a novel scanner for the in-depth analysis of polychrome surfaces’, *Optics for Art, Architecture and Archaeology, SPIE*, 8790(IV), pp. 1-9. doi: 10.1117/12.2020286.

Cucci, C. *et al.* (2015). ‘Hyperspectral remote sensing techniques applied to the non-invasive investigation of mural paintings: a feasibility study carried out on a wall painting by Beato Angelico in Florence’, *Optics for Arts, Architecture and Achaeology V*, Proc. of SPIE, 9527, 1-9. doi: 10.1117/12.2184743.

Cucci, C., Delaney, J. K. & Picollo, M. (2016). ‘Reflectance Hyperspectral Imaging for Investigation of Works of Art: Old Master Paintings and Illuminated Manuscripts’, *Accounts of chemical research*, 49, pp. 2070-2079. doi: 10.1021/acs.accounts.6b00048.

Cucci, C., *et al.* (2023). ‘A novel Transmittance Vis-NIR Hyper-Spectral Imaging scanner for analysis of photographic negatives: proof-of-concept for a new tool in photography conservation’, *Sensors*, 23(7), 3562. doi: 10.3390/s23073562.

De la Roja, J. M. *et al.* (2007). ‘Variations in the Colorimetric Characteristics of Verdigris Pictorial Films Depending on the Process Used to Produce the Pigment and the Type of Binding Agent Used in Applying it’, *COLOR research and application*, 32(5), pp. 414-423. doi: 10.1002/col.20311.

Delaney, J. K. *et al.* (2016). ‘Visible and infrared imaging spectroscopy of paintings and improved reflectography’, *Heritage Science*, 4(3), pp. 1-10. doi: 10.1186/s40494-016-0075-4.

Gil, M. *et al.* (2014). ‘Material and Diagnostic Characterization of 17th Century Mural Paintings by Spectra-Colorimetry and SEM-EDS: An Insight Look at José de Escovar Workshop at the CONVENT of Na Sra da Saudacao (Southern Portugal)’, *COLOR research and application*, 39(3), pp. 288-306. doi: 10.1002/col.21792.

Lorusso, S., Natali, A. & Matteucci, C. (2007). ‘Colorimetry applied to the field of cultural heritage: examples of study cases’, *Conservation Science in Cultural Heritage*, 7, pp. 187-220.

Marcus, R. T. (1998), ‘The measurement of color’. In: Nassau, K., Ed., ‘Color for Science, Art and Technology’, Amsterdam: Elsevier, chapter 2, pp. 31-96.

Ming, Z., Goosens, R. & Daels L. (1993). ‘Application of Satellite Remote Sensing to Soil and Land Use Mapping in the Rolling Hilly Areas of Nanjing, Eastern China’, *EARSeL Advances in Remote Sensing*, 2(3), pp. 34-43.

Mounier, A. & Daniel, F. (2017). ‘Pigment & dyes in a collection of medieval illuminations (14th-16th century)’, *Color Res Appl.,* 42, pp. 807-822. doi: 10.1002/col.22146.

Mouroulis P. *et al.* (1997). ‘Trade Studies in Multi/hyperspectral Imaging Systems Final Report’, *NASA Earth Science Technology Office USA*.

Nieke J. *et al.* (1997). ‘Imaging spaceborne and airborne sensors systems in the beginning of the next century’, *Sensors, Systems, and Next-Generation Satellites,* Proc. of SPIE, 3221, pp. 581-592. doi: 10.1117/12.298124.

Palomar, T. *et al.* (2019). ‘Analysis of chromophores in stained-glass windows using Visible Hyperspectral Imaging in-situ’, *Spectrochimica Acta Part A: Molecular and Biomolecular Spectroscopy*, 223, 1-9. doi: 10.1016/j.saa.2019.117378.

Perri A. *et al.* (2019). 'Hyperspectral imaging with a TWINS birefringent interferometer', *Optics Express*, 27(11), 15956-15967. doi: 10.1364/OE.27.015956.

Picollo, M., *et al.* (2020). 'Hyper-Spectral Imaging Technique in the Cultural Heritage Field: New Possible Scenarios', *Sensors*, 20, p. 2843. doi: 10.3390/s20102843.

Picollo, M., *et al.* (2023). 'Application of Hyper-Spectral Imaging Technique for Colorimetric Analysis of Paintings', *SCIRES-IT-SCIentific RESearch and Information Technology*, 12(2), 69-76.

Striova, J., Dal Fovo, A. & Fontana, R. (2020). 'Reflectance imaging spectroscopy in heritage science', *La Rivista del Nuovo Cimento*, 43, pp. 515-566. doi: 10.1007/s40766-020-00011-6.

Verhoeven, G. (2018). 'Multispectral and Hyperspectral Imaging', *The Encyclopedia of Archaeological Sciences*, pp. 1-4.

Vitorino, T. *et al*. (2015). 'Non-invasive identification of traditional red lake pigments in fourteenth to sixteenth centuries paintings through the use of hyperspectral imaging technique', *Applied Physics A-Materials Science Processing*, 121(3), pp. 891-901. doi: 10.1007/s00339-015-9360-4.